AAPS PharmSciTech, Vol. 16, No. 5, October 2015 (© 2015)
DOI: 10.1208/s12249-015-0300-6

Research Article

Fabrication and *In Vitro*/*In Vivo* Performance of Mucoadhesive Electrospun Nanofiber Mats Containing α-Mangostin

Wipada Samprasit,[1] Theerasak Rojanarata,[1] Prasert Akkaramongkolporn,[1] Tanasait Ngawhirunpat,[1] Ruchadaporn Kaomongkolgit,[2,3] and Praneet Opanasopit[1,3]

Received 20 July 2014; accepted 22 January 2015; published online 26 February 2015

Abstract. This study aimed to fabricate mucoadhesive electrospun nanofiber mats containing α-mangostin for the maintenance of oral hygiene and reduction of the bacterial growth that causes dental caries. Synthesized thiolated chitosan (CS-SH) blended with polyvinyl alcohol (PVA) was selected as the mucoadhesive polymer. α-Mangostin was incorporated into the CS-SH/PVA solution and electrospun to obtain nanofiber mats. Scanning electron microscopy, differential scanning calorimetry, X-ray diffraction, and tensile strength testing were used to characterize the mats. The swelling degree and mucoadhesion were also determined. The nanofiber mats were further evaluated regarding their α-mangostin content, *in vitro* α-mangostin release, antibacterial activity, cytotoxicity, *in vivo* performance, and stability. The results indicated that the mats were in the nanometer range. The α-mangostin was well incorporated into the mats, with an amorphous form. The mats showed suitable tensile strength, swelling, and mucoadhesive properties. The loading capacity increased when the initial amount of α-mangostin was increased. Rapid release of α-mangostin from the mats was achieved. Additionally, a fast bacterial killing rate occurred at the lowest concentration of nanofiber mats when α-mangostin was added to the mats. The mats were less cytotoxic after use for 72 h. Moreover, *in vivo* testing indicated that the mats could reduce the number of oral bacteria, with a good mouth feel. The mats maintained the amount of α-mangostin for 6 months. The results suggest that α-mangostin-loaded mucoadhesive electrospun nanofiber mats may be a promising material for oral care and the prevention of dental caries.

KEY WORDS: dental caries; mucoadhesive property; nanofibers; thiolated chitosan; α-mangostin.

INTRODUCTION

The mouth, or oral cavity, contains oral bacteria, including streptococci, lactobacilli, staphylococci, corynebacteria, and various anaerobes, and particularly *Bacteroides*. Several of these species are considered commensal and are believed to positively affect oral health, whereas others are considered pathogenic (1). When the oral environment changes, the proliferation of various pathogenic species at different sites in the mouth may increase hazardously and may initiate and further aggravate certain oral diseases. *Streptococcus mutans* and *Streptococcus sanguinis* rapidly colonize and appear on the dental surface and gingiva. These two types of bacteria are associated with the occurrence of human dental caries (2). These bacteria have the ability to utilize sugars, resulting in the production of acids that eventually dissolve the hard, crystalline structure of the teeth, resulting in carious lesions (3). Moreover, both species have the ability to synthesize extracellular glucans, which are the major factors in the development of cariogenic biofilms (4). Several *Lactobacillus* spp. have been associated with dental caries, although these bacteria are normally symbiotic in humans and found in the gut flora (5).

Important components of the maintenance of good dental health, together with reduction of the individual risk of dental caries, are avoidance of frequent consumption of carbohydrates between meals, as well as tooth brushing and flossing (6). In the case of high caries risk, the use of mouthwash and fluoride is recommended (7). However, many researchers have discovered and developed antibacterial agents and dosage forms to maintain oral hygiene and prevent dental caries by eradication of bacterial pathogens, especially in the case of individuals heavily colonized by *S. mutans*. α-Mangostin has been reported to have active antimicrobial activity against *Staphylococcus aureus* and *Enterococcus* spp. (8,9). These two pathogens are associated with the occurrence of oral and dental disorders. However, α-mangostin has never been reported to have activity against human dental caries pathogens, i.e., *S. mutans*, *S. sanguinis*, and *Lactobacillus* spp.

Recently, buccal mucosal drug delivery has attracted interest due to its suitability for the administration of retentive dosage forms (10). To achieve buccal adhesion, an appropriate mucoadhesive polymer must be used. The biopolymer chitosan (CS) has been proposed for use in oral mucosal drug

[1] Pharmaceutical Development of Green Innovations Group (PDGIG), Faculty of Pharmacy, Silpakorn University, Nakhon Pathom, 73000, Thailand.
[2] Department of Oral Diagnosis, Faculty of Dentistry, Naresuan University, Phitsanulok, 65000, Thailand.
[3] To whom correspondence should be addressed. (e-mail: ruchadapornk@yahoo.com)

delivery (11), and thiolation of CS can lead to improvement of the mucoadhesion of unmodified CS (12). The free thiol groups on the polymeric backbone are capable of forming covalent bonds with the cysteine residues of mucins, which creates the interactions necessary for mucoadhesion (13,14). Polyvinyl alcohol (PVA) also presents adhesive force due to the formation of hydrogen bonding with the mucus. In a previous study, we successfully developed *Garcinia mangostana* (GM) extract-containing mucoadhesive electrospun nanofiber mats using CS and thiolated CS (CS-SH) as mucoadhesive polymers. We found that CS-SH significantly improved the mucoadhesive property of the mats in comparison with unmodified CS (15). Thus, the use of CS-SH and PVA for buccal mucosal dosage forms is of interest.

There are many buccal mucosal formulations, e.g., tablets, films, and hydrogels. One interesting formulation is films due to their small size and reduced thickness compared with tablets, for example (16). Films contain a surface layer possessing adhesive properties. Film casting and hot-melt extrusion are the processes used to manufacture films. The film-casting process involves casting of a solution to yield films. As an alternative, hot-melt extrusion is a process that forces the blending of melted polymers to create films. Nanofiber mats look similar to films, but the polymers are arranged in the nanorange of diameters. These mats have several amazing characteristics, such as a large surface area-/volume ratio (high contact surface area) and good flexibility (17), which not only enhance the dissolution rate but also increase the total amount of drug released from drug-loaded nanofiber mats compared with films of the same composition. These outstanding properties make nanofiber mats optimal candidates for buccal mucosal formulations. The mucoadhesive property and the characteristics of nanofibers encourage a high drug concentration at the site of active local drug delivery. A number of processing techniques, including drawing, template synthesis, phase separation, self-assembly, and electrospinning, have been used to prepare nanofiber mats (17). Electrospinning has been intensively used to prepare nanofiber mats. The simplicity of one continuous step is an attractive benefit of this process. Therefore, in the current study, the electrospinning technique was selected to fabricate mucoadhesive electrospun nanofiber mats containing α-mangostin for the maintenance of oral hygiene and reduction of the bacterial growth that causes dental caries. In this study, CS-SH was synthesized, blended with PVA, and electrospun to obtain the nanofiber mats. The morphology and physical and mechanical characteristics of the mats were observed. The mats were evaluated for properties that included the amount of α-mangostin; swelling; mucoadhesion; *in vitro* release; *in vitro* antibacterial activity; cytotoxicity; stability; and *in vivo* antibacterial activity, mucoadhesive properties, and taste and mouth feel.

MATERIALS AND METHODS

Materials

CS (degree of deacetylation, 0.85; MW, 110 kDa), ethylenediaminetetraacetic acid (EDTA), cysteine hydrochloride, 1-ethyl-3-(3-dimethylaminopropyl) carbodiimide hydrochloride (EDAC), 5, 5′-dithio-bis-(2-nitrobenzoic acid) (DTNB), 3-(4,5-dimethylthiazol-2-yl)-2,5-diphenyl-tetrazolium bromide (MTT), and α-mangostin were purchased from Sigma-Aldrich Chemical Company, USA. PVA (degree of polymerization ≈ 1600; degree of hydrolysis ≈ 97.5–99.5 mol.%) was purchased from Fluka, Switzerland. Brain heart infusion (BHI; BBL™, MD, USA), mitis salivarius agar, and lactobacillus de Man–Rogosa–Sharpe (MRS) agar (Difco, USA) were purchased and used as received. Dulbecco's modified Eagle'smedium (DMEM), fetal bovine serum (FBS), Trypsin–EDTA, L-glutamine, penicillin, streptomycin, and amphotericin B were purchased from GibcoBRL (Grand Island, NY, USA). All other reagents and solvents were commercially available and were of analytical grade.

Methods

Preparation of α-Mangostin

α-Mangostin was received from the Department of Pharmacognosy and Pharmaceutical Botany, Faculty of Pharmaceutical Sciences, Chulalongkorn University, Thailand. The purified α-mangostin was prepared according to the protocol of a previous study (18). Briefly, the pericarp of mangosteen was macerated in hexane to remove nonpolar compounds and was subsequently macerated in ethyl acetate. α-Mangostin was obtained from the crude extract by chromatography on a silica gel column and elution with hexane/ethyl acetate (4:1). The selected fraction was identified as α-mangostin (Fig. 1a) using mass spectrometry, nuclear magnetic resonance spectroscopy, and a Gallenkamp melting-point apparatus.

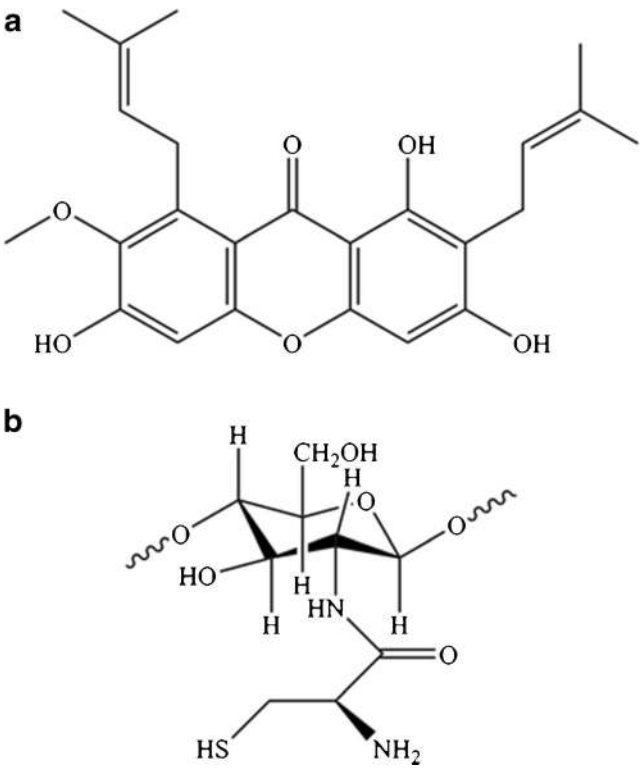

Fig. 1. The chemical structure of **a** α-mangostin and **b** CS-SH

Synthesis of Thiolated Chitosan

CS-SH was synthesized following the preparation procedures as applied in CS-*N*-acetyl cysteine conjugation (19). Cysteine hydrochloride was dissolved in deionized water, and its carboxylic acid moieties were activated by 150 mM EDAC for 20 min. The activated cysteine hydrochloride was added to a solution of CS in 1% *v*/*v* HCl. The pH was adjusted to within the range of 4–5 with 2 N NaOH and was maintained during the experiment. The solution was stirred for 6 h, and the CS-SH was then isolated in the dark by dialysis with 1 mM HCl and 1% *w*/*v* NaCl for 3 days (molecular weight cut-off of dialysis membrane=12–14 kDa). The product was pre-frozen at −80°C for 12 h and was then dried under high vacuum for 3–4 days (FreeZone 2.5, Labconco, UK).

The amount of free thiol groups on the CS-SH was determined photometrically with Ellman's reagent. In total, 10 mg of CS-SH was hydrated with 750 μl of 0.1 M phosphate buffer (pH 8) and 1 mM EDTA. Then, 250-μl aliquots were added to 2.5 ml of 0.1 M phosphate buffer (pH 8) and 1 mM EDTA or to 50 μl of Ellman's reagent [4 mg of DTNB dissolved in 1 ml of 0.1 M phosphate buffer (pH 8) and 1 mM EDTA]. The reaction was allowed to proceed for 15 min at room temperature, and the absorbance was measured at a wavelength of 412 nm (Agilent Technologies, USA). The amount of free thiol groups was calculated from the corresponding cysteine standard curve, elaborated between 0.20 and 0.8 mM cysteine hydrochloride.

Fabrication of Mucoadhesive Electrospun Nanofiber Mats Containing α-Mangostin

A 2% *w*/*v* CS-SH solution was prepared by dissolving CS-SH plus EDTA in distilled water at a weight ratio of 2:1. A 10% *w*/*v* PVA solution was prepared by dissolving PVA in distilled water at 80°C and then allowing the solution to stir for 4 h. The electrospinning solution was prepared by mixing the CS-SH solution and the PVA solution at a weight ratio of 30:70. Various amounts of α-mangostin (% *w*/*w* α-mangostin to polymer) were added to the CS-SH/PVA solution by stirring for 24 h. The pH of the polymer solution was 4.0. The solution's viscosity, conductivity, and surface tension were measured before preparing nanofiber mats via the electrospinning process. The solution was contained in a 5-ml glass syringe connected to a 20-gauge, stainless steel needle (diameter=0.9 mm) at the nozzle. The needle was connected to the emitting electrode of a positive-polarity (Gamma High Voltage Research, FL, USA) device. The electric potential was fixed at 15 kV. The nanofiber mats were collected as spun on aluminum foil that covered a rotating collector at a speed of 400 m/min. The electrospinning process was conducted at 25°C and 60% relative humidity (RH), and the collection distance was fixed at approximately 20 cm. The solution feeding rate was fixed at 0.45 ml/h using a syringe pump (Model NE-300, New Era Pump Systems Inc.) during processing.

Characterization of Mucoadhesive Electrospun Nanofiber Mats Containing α-Mangostin

The morphology and diameter of the nanofiber mats were examined using scanning electron microscopy (SEM; Camscan Mx2000, England). A small section of the nanofiber mats was sputtered with a thin layer of gold before SEM observation. The average diameter of the nanofiber mats was determined using image analysis software (JMicroVision V.1.2.7, Switzerland), with 50 measurements collected from the SEM image of each sample.

Powder X-ray diffraction (XRD) was performed to investigate the physical state of the α-mangostin in the nanofiber mats using a vertical type of X-ray powder diffractometer (MiniFlex II, Rigaku Co., Japan). Each sample was irradiated with monochromatized Cu Kα radiation after passage through nickel filters and was then analyzed between 5 and 45° (2θ) at room temperature. The scanning speed, time, voltage, and current applied were 4.0°/min (2θ), 10 min, 30 kV, and 15 mA, respectively.

The thermal behavior of the nanofiber mats was determined using differential scanning calorimetry (DSC; Pyris Diamond DSC, PerkinElmer, USA). Each sample (2–4 mg) was placed in an aluminum pan, and the cover was crimped to provide a hermetically sealed sample. The heating rate was 10°C/min. All measurements were obtained at over 25–300°C under nitrogen flow at 20 ml/min.

The tensile strength of the nanofiber mats was evaluated using a texture analyzer (TA.XTplus, Stable Micro Systems, UK) with a 5-kg load cell equipped with tensile grips. The nanofiber mats were cut into a rectangular shape (6×35 mm). The thicknesses of these samples ranged from 20 to 30 μm. The speed was 0.5 mm/s, and the temperature was 25°C.

Swelling Degree of Nanofiber Mats

The swelling degree of the nanofiber mats was investigated in 2 ml of artificial saliva (pH 6.8) at room temperature for 1 h and calculated according to Eq. 1:

$$\text{Degree of swelling}(\%) = \frac{(M - M_d)}{M_d} \times 100 \quad (1)$$

where M is the weight of the nanofiber mats after immersion in the buffer solution for 1 h, and M_d is the initial weight of the nanofiber mats in their dry state.

Mucoadhesive Property of Nanofiber Mats

A measurement of mucoadhesion was performed according to the protocol of a previous study, with slight modification (20). The mucoadhesive force of the nanofiber mats on porcine buccal mucosa was assessed using a texture analyzer with a 50-N load cell and equipped with a mucoadhesive holder. The nanofiber mats were cut into a rectangular shape (10×10 mm) and attached to the aluminum probe (10 mm in diameter) using a double-sided adhesive tape. Freshly excised porcine buccal mucosa was put in Kreb's buffer and thawed at the time of use by incubation at 37±0.5°C for 15 min. The tissue was securely placed onto the holder stage of the mucoadhesive holder. Then, 500 μl of artificial saliva was added to the center of the buccal mucosa and instantly spread over the whole surface. Upon contact between the nanofiber mat and the buccal mucosa, a constant force (3 g) was applied for 1 min. The mucoadhesive performance was determined by

measuring the resistance to withdrawal of the probe, causing the nanofiber mats to detach from the tissue (maximum detachment force), reflecting the mucoadhesive force of the nanofiber mats. The force was recorded using Texture Exponent 32 software.

α-Mangostin Content

The amount of α-mangostin in a nanofiber mat was determined by submerging an accurately weighed mat (1 mg) in 1 ml of methanol for 24 h. The α-mangostin content was then analyzed using high performance liquid chromatography (HPLC) (Agilent Technologies, USA). A VertiSep® AQS C18 column (250×4.6 mm, 5 μm particle size) with a C18 guard column was used. In total, 20 μl of the submerging solution was injected and analyzed by HPLC, which was performed according to a previously reported method, with slight modification (21). Elution was performed using gradient solvent systems that consisted of acetonitrile (mobile A) and 0.1% *v*/*v* orthophosphoric acid (mobile B) with a flow rate of 1 ml/min at ambient temperature. The gradient program was as follows: 70% A for 0–15 min, 70% A to 75% A in 3 min, 75% A to 80% A in 1 min, constant at 80% A for 6 min, and 80% A to 70% A in 1 min. There was 10 min post-run for reconditioning. The wavelength of the ultraviolet–visible (UV–vis) detector was set at 320 nm. The amount of α-mangostin in the mats was calculated using the calibration curve for α-mangostin. A solution of α-mangostin was prepared by dissolving an accurately weighed amount (10 mg) of α-mangostin in 10 ml of methanol in a volumetric flask. Various concentrations of α-mangostin were diluted to obtain final concentrations in the range of 5–200 μg/ml in methanol. The loading efficacy (%) and loading capacity (%) of α-mangostin were calculated using Eqs. 2 and 3, respectively:

$$\text{Loading efficacy}(\%) = \left(\frac{L_a}{L_t}\right) \times 100 \tag{2}$$

$$\text{Loading capacity}(\%) = \left(\frac{L_a}{W}\right) \times 100 \tag{3}$$

where L_a is the amount of α-mangostin that was embedded in the nanofiber mat, L_t is the theoretical amount of α-mangostin (obtained from the feeding condition) incorporated into the nanofiber mat, and W is the weight of the nanofiber mat.

In Vitro Release of α-Mangostin

α-Mangostin release was investigated in a 10-ml solvent mixture of artificial saliva and methanol (50:50). In total, 10 mg of nanofiber mats, which was equivalent to 60, 180, and 300 μg of α-mangostin for the 1, 3, and 5% α-mangostin-loaded mats, respectively, was weighed and placed into release medium. The medium was maintained at 37±0.5°C while being shaken at 150 rpm throughout the test. At a given time point, an aliquot of 1 ml of the sample solution was withdrawn and replaced with the same volume of fresh medium to maintain a constant volume. The amount of α-mangostin in the sample solutions was then analyzed by HPLC. The obtained data were carefully assessed to determine the cumulative amount of α-mangostin release from the specimens at each immersion time point.

Release Kinetics of Nanofiber Mats

The release kinetics of the α-mangostin-loaded nanofiber mats were investigated using a zero-order model, a first-order model, and the Higuchi model, as follows:

1. Zero-order model
   The data obtained from *in vitro* drug release studies were plotted as cumulative amounts of drug released (Q_t) *vs.* time. This model, shown by Eq. 4, describes the drug release pattern, assuming that the drug release rate is independent of its concentration (22):

$$Q_t = k_0 t \tag{4}$$

where Q_t is the amount of drug released at time t; k_0 is the zero-order release constant, expressed in units of concentration/time; and t is the time.

2. First-order model
   The data obtained were plotted as the log of the cumulative percentage of drug remaining *vs.* time. This model, shown by Eq. 5, describes the drug release pattern, assuming that the drug release rate is dependent on its concentration (23):

$$\log C = \log C_0 - \frac{kt}{2.303} \tag{5}$$

where C_0 is the initial concentration of the drug, k is the first-order rate constant, and t is the time.

3. Higuchi model
   This model describes drug release from a matrix system as a process that is dependent on the square root of time, based on Fickian diffusion, as in Eq. 6:

$$Q = kt^{1/2} \tag{6}$$

where Q is the cumulative amount of drug released at time t, K is the Higuchi release rate constant, and t is the time. A straight line can be obtained by plotting Q *vs.* t. The resultant slope is the Higuchi rate constant (24).

In Vitro Antibacterial Activity of Nanofiber Mats

Susceptibility Test. The antibacterial activity of the nanofiber mats was tested against *S. mutans* A32-2 and *S. sanguinis* ATCC 10556 using a broth dilution technique (25). The minimum inhibitory concentration (MIC) and the minimum bactericidal concentration (MBC) values were determined. All strains were grown and cultured at 37°C in a 5% CO_2 atmosphere in BHI broth for 24 h before use. The culture of each bacterial strain was adjusted to 1–2×10^6 colony-forming units (CFU)/ml. Sterilized mats (UV radiation for 1 h) were then added to the bacterial suspensions at 0.1, 0.2, 0.5, 1, 2, 3, 4, or 5 mg/ml. After 24 h of incubation, the bacterial suspensions were observed for turbidity. The MIC was defined as the lowest concentration that presented a clear well, with an absence of turbidity by visual inspection. A 100-μl aliquot from dilution tubes without turbidity was inoculated on BHI agar

plates. The plates were then incubated to allow bacterial growth for 24 h. The MBC was defined as the lowest concentration that reduced the number of viable bacteria by 99.9% (26). BHI broth with bacterial suspension served as the negative control, and 0.2% *w/v* chlorhexidine was used as the positive control.

Time Kill Assay. The rate of bactericidal activity was examined by time-kill assay. Cell suspensions of *S. mutans* and *S. sanguinis* were separately cultured in BHI broth and adjusted to $1–2\times10^6$ CFU/ml. The bacterial suspensions were treated with nanofiber mats at a fixed concentration (the MBC of the blank nanofiber mats). A 100-µl aliquot of each sample was collected after 0, 30, 60, 120, 180, and 240 min of incubation. Serial 10-fold dilutions of the samples were performed in BHI broth (10^1-, 10^2-, and 10^3-fold) were performed, and 100-µl aliquots from the dilution tubes were inoculated on BHI agar plates by the spread plate method. The numbers of viable bacteria were counted after incubation for 24–48 h. Cultivation of bacteria in BHI broth alone or with 0.2% *w/v* chlorhexidine were used as the negative and positive controls, respectively, for bacterial growth at each time point. The number of viable colonies of each strain was calculated to determine CFU/ml, and a graph of time *vs.* the number of viable colonies was plotted.

Cytotoxicity

The cytotoxicity of α-mangostin and the α-mangostin-loaded nanofiber mats was evaluated using a human keratinocyte cell line (HaCaT) and human gingival fibroblasts (HGFs) in the MTT assay. The HGFs were obtained from explants of gingival tissue attached to non-carious, freshly extracted third molars. All patients gave informed consent for tissue collection. Ethical approval for the study was obtained from Naresuan University's Institutional Review Board (COE No. 55 02 04 0024). The cells were cultured in DMEM supplemented with 10% FBS, 2 mM L-glutamine, 100 IU/ml penicillin, 100 µg/ml streptomycin, and 5 µg/ml amphotericin B at 37°C in a humidified atmosphere of 95% air and 5% CO_2. The α-mangostin and nanofiber mats were sterilized by UV radiation for 1 h before testing. Each cell type was seeded at 25,000 cells per well in 48-well plates. When the cultures reached confluence, they were treated with α-mangostin at concentrations ranging from 0 to 1 µg/ml in serum-free medium (SFM), with subsequent incubation for 24 h. For the nanofiber mats, when the cultures reached confluence, the SFM was replaced, and the nanofiber mats were then added to the wells. The cells were incubated for 15, 30, 60, 120, or 240 min. The tests on the nanofiber mats also determined the long-term cytotoxicity by rinsing the cells with phosphate buffer (pH 7.4) at the end of testing. The SFM was then replaced, and the cells were reincubated for 24, 48, or 72 h. After treatment, the cytotoxicity was examined by MTT assay. The cells were incubated with 200 µl of an MTT solution (0.5 mg/ml in DMEM without phenol red) in a CO_2 incubator for 1 h. The solution was then removed, and 500 µl of DMSO was added to dissolve the formazan crystals. The amount of purple formazan crystal formation was proportional to the number of viable cells. The cell viability (%) was calculated based on the absorbance at 570 nm using a Genesys 10S UV–vis spectrophotometer (Thermo Scientific, New York, USA). The viability of non-treated control cells was arbitrarily defined as 100%.

In Vivo Study

An *in vivo* study was performed in six healthy human volunteers to evaluate the antibacterial activity, mucoadhesive property, and taste and mouth feel of the nanofiber mats. Blind testing was selected for this study. This study was approved by an institutional review board (Human Studies Ethics Committee, Faculty of Pharmacy, Silpakorn University, approval no. 9-2556). The volunteers had no signs of any oral disease, no evidence of gingivitis, and an absence of active caries. None of the subjects had received antibiotics or topical antiseptics during the previous 30 days or had systemic disease that would have altered the amount or composition of saliva. Each volunteer was administered one nanofiber mat at a weight of 4 mg. The mat was adhered to the buccal mucosa, and then the period of adhesion was recorded as the *in vivo* adhesion time. Non-stimulated saliva samples (2 ml) were collected from each participant using the spitting method at baseline, 15, 30, and 60 min during the experiments. The bitterness and mouth feel (grittiness or smoothness) were simultaneously observed during the test. Afterward, the volunteers rinsed their oral cavity with water, without swallowing the disintegrated material. The 2 ml samples of saliva were reserved for microbiological measurements following dilution with phosphate buffer at pH 6.8. Aliquots of the dilution were spread on mitis salivarius agar and lactobacillus MRS agar. The plates were incubated in an atmosphere of 5% CO_2 at 37°C for 48 h, and the viable colonies were assessed. The number of bacteria at baseline was arbitrarily defined as 100% and served as the control. A graph of time *vs.* the number of viable bacteria was plotted, and the number of viable cells at each time point was expressed as a percentage of the number of bacteria at baseline.

Stability Studies

The stability of the nanofiber mats was monitored according to ICH guidelines for long-term conditions (25±2°C and 60±5% RH) comparing with accelerated conditions (40±2°C and 75±5% RH) for 6 months. The content of α-mangostin was observed after 1, 3, and 6 months.

Statistical Analysis

All experimental measurements were collected in triplicate. Data were expressed as the mean±standard deviation (SD). The statistical significance of the difference in numbers of viable bacteria of time-kill assay and percent cell viability of cytotoxicity test were examined using one-way analyses of variance (ANOVA), followed by a least significant difference (LSD) post hoc test and Student's *t* test, respectively. The significance level was set at $p<0.05$.

RESULTS AND DISCUSSION

Synthesis of CS-SH

CS-SH was successfully synthesized by the formation of amide bonds (27). The carboxylic acid moieties of cysteine were activated by EDAC, which reacted with the primary amino groups of CS. Figure 1b, which was modified from a review by Sreenivas and Pai (27), shows the chemical structure of CS-SH. After lyophilization, the CS-SH appeared as a white and odorless powder with a fibrous structure. The amount of free thiol groups, which was determined with Ellman's reagent, was 469.75±2.82 μmol/g of polymer. According to the result, 8.3% of all primary amino groups on CS formed amide bonds with cysteine.

Electrospinning of Mucoadhesive Nanofiber Mats

CS-SH/PVA solutions containing various amounts of α-mangostin (0, 1, 3, or 5% *w*/*w* α-mangostin to polymer) were prepared. The solution parameters, including viscosity, conductivity, and surface tension before electrospinning, were determined and are listed in Table I. The amount of α-mangostin added to the solution affected the morphology of the nanofiber mats, as presented in Fig. 2. The images show that all mats were smooth in the nanometer range, without apparent crystals of α-mangostin in the structure. Non-beaded nanofiber morphology was also observed. These results indicated that the α-mangostin was well incorporated within the mats. The diameters of the nanofibers are also presented in Fig. 2. The blank nanofiber mats had the smallest diameter size (Fig. 2a). By increasing the α-mangostin content from 1 to 5%, the nanofiber diameter increased due to the increased viscosity and reduced conductivity of the solution, whereas the surface tension was not different (Table I). This information is significantly related to morphological changes in nanofiber mats (28,29). When viscosity is increased, which indicates a greater amount of polymer chain entanglement in a solution, the electrospinning jet will be able to fully stretch the solution, with the solvent molecules distributed among the polymer chains, causing the nanofiber diameter to increase (30). Additionally, the decrease in conductivity reduces the charge-carrying capacity of the solution, thereby subjecting it to lower tension in the applied electric field and an increase in the diameter of the nanofibers (29). Nevertheless, the morphology of the α-mangostin-loaded nanofiber mats was smooth and uniform, and the diameter ranged between 163 and 166 nm. Moreover, there were spaces between each fiber in all nanofiber mats, indicating their porosity (Fig. 2). Therefore, the α-mangostin was favorably incorporated into the nanofiber mats and was further characterized and evaluated regarding mucoadhesive dosage forms.

Table I. Solution Parameters of Electrospinning Solutions Containing Various Amounts of α-Mangostin

α-Mangostin (% *w*/*w*)	Viscosity (mPa s)	Conductivity (μS/cm)	Surface tension (mN/m)
0	230.37±0.65	2363.3±55.1	54.48±1.22
1	242.27±0.57	2260.0±20.0	57.24±0.61
3	252.90±3.15	2220.0±43.6	58.40±0.09
5	265.93±3.31	1998.0±149.3	58.30±0.03

Characterization of Mucoadhesive Nanofiber Mats

The X-ray patterns of α-mangostin powder and the nanofiber mats are displayed in Fig. 3a. The diffractogram of α-mangostin exhibited strong, sharp peaks, indicating that α-mangostin was present in crystalline form. However, no such peaks were found in the diffractograms of blank and α-mangostin-loaded nanofiber mats. The disappearance of the α-mangostin crystalline peaks indicated that α-mangostin was well incorporated in the mats and converted from its crystalline state to an amorphous state.

A DSC experiment further characterized the physical state of α-mangostin in the electrospun nanofiber mats, and the thermograms are illustrated in Fig. 3b. The thermogram of α-mangostin displayed a sharp endothermic peak at 180°C due to its melting point. A broad peak in the endothermic curve of the blank nanofiber mats was also observed at 192.21°C, which indicated its melting point. The melting points of the mats slightly increased, from approximately 192°C to 200°C, when the amount of α-mangostin increased. The shift observed may have been due to an interaction between α-mangostin and the nanofiber mats. In addition, the absence of the melting α-mangostin peak for the mats demonstrated that α-mangostin was incorporated into the mats in its amorphous state. During the electrospinning process, the CS-SH/PVA solution inhibited the recrystallization of α-mangostin. In addition, the melting peak and thermogram profile of the blank nanofiber mats were shifted to a higher temperature (192–200°C) than for the α-mangostin-loaded nanofiber mats, evidencing an interaction between α-mangostin and the CS-SH/PVA polymer.

Table II exhibits the mechanical properties of the mucoadhesive nanofiber mats, which are an important factor for handling and storage. The tensile strength was measured to represent the mechanical strength of the mats. This parameter represents the resistance of the nanofiber mats to a force tending to tear it apart, measured as the maximum tension that the mats could withstand without tearing (10). The tensile strength of all mats was in the range of 4.24–4.60 MPa. These results indicated that the loaded α-mangostin exerted a limited effect on the mechanical properties of the mats. All mats had a tensile strength high enough to withstand tearing during handling and storage.

Swelling Degree and Mucoadhesive Property

Swelling is an important property that can indicate the mucoadhesion of dosage forms. Sufficiently mucoadhesive nanofiber mats should swell at the interface between the mats and the epithelial/mucus layer. When a nanofiber mat capable of rapid gelation in an aqueous environment is brought into contact with gel, water movement occurs between gels until equilibrium is achieved and brought into contact with mucus gels (31). The swelling degree of the nanofiber mats after immersion in artificial saliva for 1 h is displayed in Table II. The blank nanofiber mats provided the highest swelling degree (195.75±11.95%), which decreased with increasing amounts of loaded α-mangostin. Swelling degrees of 160.26, 80.14, and 69.51% were noted for the mats containing 1, 3, and

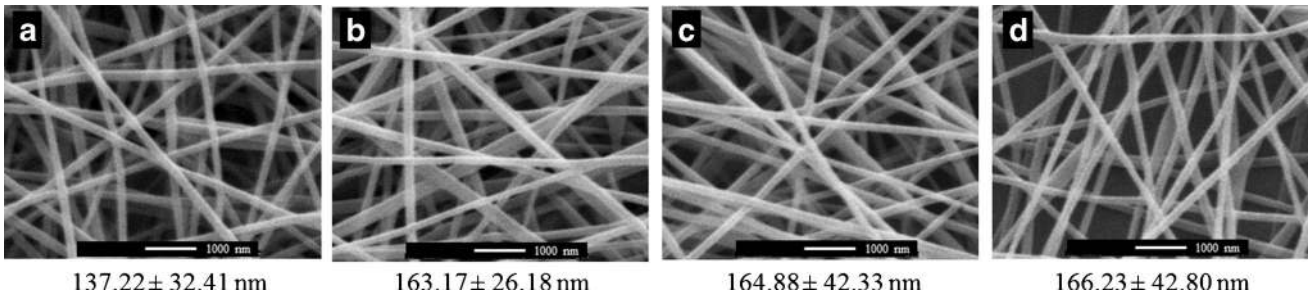

Fig. 2. The SEM images (10,000×) and diameter of the mucoadhesive nanofiber mats containing different amounts of α-mangostin: **a** 0, **b** 1, **c** 3, and **d** 5% *w/w* to polymer

5% α-mangostin, respectively. The CS-SH and PVA in the mats are hydrophilic, encouraging rapid water diffusion and polymer swelling. In contrast, α-mangostin is a hydrophobic compound, so it might have caused the decrease in the swelling degree by increasing the hydrophobicity of the nanofiber mats. Nonetheless, the mucoadhesive property did not directly vary with the degree of swelling. All mats exhibited an insignificant difference in the mucoadhesive force (Table II). The maximum force required for separation of the nanofiber mats from porcine buccal mucosa was approximately 22 g. These results indicated that the loaded α-mangostin reduced the swelling property without affecting the mucoadhesive property. The free thiol groups of the CS-SH introduced a sulfhydryl group for crosslinking with cysteine-rich mucus glycoprotein via disulfide bonds (32). This interaction caused direct adhesion to the cell surface; thus, α-mangostin had a limited effect on the mucoadhesive property. Indeed, PVA itself has a mucoadhesive property via non-covalent interactions, i.e., hydrogen bonds and hydrophobic interactions, so it might also have partly caused the mucoadhesion of the nanofiber mats.

α-Mangostin Content

Various amounts of α-mangostin were loaded into nanofiber mats, and actual amounts were determined and are listed in Table II as the loading efficacy (%) and loading capacity (%). The loading efficacy of α-mangostin in the mats was 61.67–66.72%, revealing that approximately 60% of an initial amount of α-mangostin could be loaded into the nanofiber mats. This was due to the limited incorporation of α-mangostin into the mats, as free α-mangostin has low aqueous solubility (0.2 μg/ml) (33). However, an increase in the initial amount of α-mangostin caused an overall increase in the amount of α-mangostin in the mats. The loading capacity increased from 0.65 to 3.18% when the α-mangostin loading was increased from 1 to 5%.

In Vitro Release Study and Release Kinetics

The profiles of α-mangostin release from the mats are displayed in Fig. 4. All mats showed similar release patterns, even though the initial amount of α-mangostin in the nanofiber mats was different. Burst release of α-mangostin from the nanofiber mats was observed. The cumulative release reached 80% within 60 min. After this time, α-mangostin continued to be released, with complete release occurring within 240 min. This result demonstrated that α-mangostin was easily released from nanofiber mats containing various concentrations of α-mangostin. When the mats were immersed in release medium, the water penetrated into the nanofiber mats, after which the α-mangostin was solvated, diffused, and released.

A release kinetics study was performed to gain further insight into the mechanism. The release kinetics of the nanofiber mats were examined by fitting with zero-order, first-order, and Higuchi models. It was found that the release profiles were best fit by the Higuchi model (R^2>0.98), as shown in Table III, indicating that the kinetics of the release of α-mangostin from the nanofiber mats was governed by the Higuchi model. This finding might be explained by

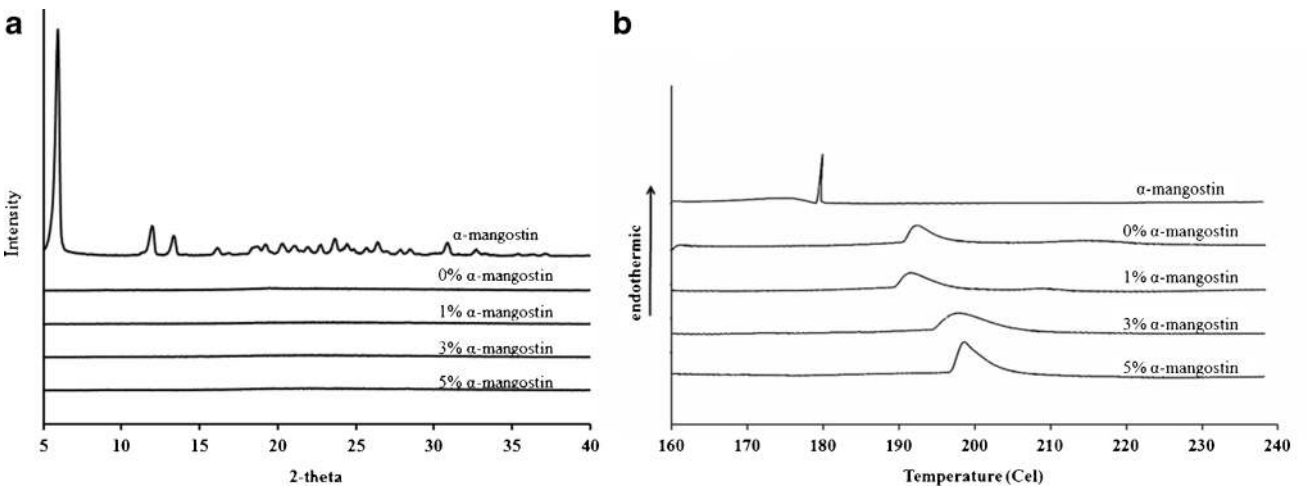

Fig. 3. The **a** X-ray patterns and **b** DSC thermograms of α-mangostin and the mucoadhesive nanofiber mats containing different amounts of α-mangostin

Table II. Characteristics of the Mucoadhesive Nanofiber Mats Containing Different Amounts of α-Mangostin

Nanofiber mats (% *w/w* α-mangostin)	Tensile strength (MPa)	Degree of swelling (%)	Mucoadhesive force (g)	Loading efficacy (%)	Loading capacity (%)
0	4.60±0.36	195.75±11.95	22.62±0.04	–	–
1	4.60±0.34	160.28±18.37	22.45±0.21	65.97±0.16	0.65±0.01
3	4.24±0.26	80.14±29.63	22.49±0.14	61.76±0.03	1.80±0.01
5	4.30±0.41	69.51±21.44	22.49±0.07	66.72±0.17	3.18±0.01

the fact that the main mechanism of α-mangostin release is diffusion (34). The fast release of α-mangostin from the nanofiber mats was also caused by the high surface area and porosity of the mats (35). Furthermore, the electrospinning process left the α-mangostin in an amorphous state, facilitating drug dissolution in the medium.

In Vitro Antibacterial Activity

The antibacterial activity of the CS-SH/PVA nanofiber mats containing various amounts of α-mangostin was tested against *S. mutans* and *S. sanguinis* using the broth dilution technique. The mats were submerged in bacterial suspension for 24 h to determine the MIC and MBC values. All mats provided effective antibacterial activity, with MIC and MBC values (Table IV) that indicated α-mangostin concentration-dependent antibacterial activity. Lower MIC and MBC values were detected when the amount of loaded α-mangostin was increased. The 1, 3, and 5% α-mangostin-loaded nanofiber mats inhibited *S. mutans* and *S. sanguinis* growth at 2, 1, and 0.5 mg/ml, respectively. The concentration required for destruction of the bacterial cells was higher than the inhibitory concentration. The MBC values were 3, 2, and 1 mg/ml for the mats containing α-mangostin at 1, 3, and 5%, respectively. These results indicated that the mats were bacteriostatic at low concentrations and bactericidal at higher concentrations (36). The mechanism of α-mangostin's induction of bacterial inhibition and destruction was mainly targeted to the cell membrane. This compound induced rapid dissipation of the membrane potential, caused structural damage to the cytoplasmic membrane, and subsequently caused considerable leakage of intracellular components (37). The blank nanofiber mats also inhibited and killed the bacterial cells. The CS-SH and EDTA contained in the mats mainly exhibited antibacterial activity. The CS-SH did not completely conjugate with cysteine; certain cationic charge on the amino groups can interfere with the anionic components of bacterial cells (38). EDTA can inhibit the growth of bacteria by inhibiting many enzymes that require cations as cofactors, i.e., Mg^{2+}, Ca^{2+}, and Fe^{2+} (39). However, the MIC and MBC of the blank nanofiber mats were higher than those of the mats containing α-mangostin (Table IV), indicating the benefit of the loaded α-mangostin in enhancing antibacterial activity.

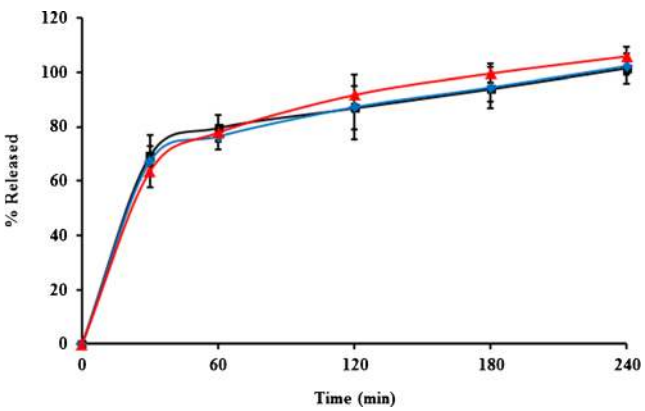

Fig. 4. The release profiles of α-mangostin from the mucoadhesive nanofiber mats containing different amounts of α-mangostin: *square* 1, *diamond* 3, and *triangle* 5% *w/w* to polymer

The antibacterial activity of the α-mangostin-loaded mucoadhesive nanofiber mats as also evaluated by counting the viable cells in *S. mutans* and *S. sanguinis* suspensions after contact with the mats. The results are illustrated as time-kill plots in Fig. 5. The rate of bactericidal activity was examined by time-kill assay as previously described, with slight modification (40). The concentration of all mats was fixed at the MBC of the blank nanofiber mats (4 mg/ml) to determine the effect of α-mangostin on the killing rate. Cultivation of bacteria alone was used as the negative control, with growth increasing as a function of time. Conversely, 0.2% chlorhexidine was used as the positive control; the bacterial cells were rapidly killed, within 30 min (Fig. 5). Meanwhile, the bacterial cells were inhibited and killed by all mats within 240 min of contact. When the contact time was increased, the CS-SH and PVA began to erode, and the α-mangostin was increasingly released, interacting with the bacterial cells. Additional α-mangostin in the mats seemed to decrease the viable cell number in the case of *S. mutans* (Fig. 5a). The 1, 3, and 5% α-mangostin-loaded nanofiber mats exhibited significantly faster *S. mutans* killing activity than the blank nanofiber mats did at 30, 60, and 120 min. However, there was no significant difference in the viable cell number between the 1, 3, and 5% α-mangostin-loaded mats at these time points. These results indicated that the benefit of the loaded α-mangostin was not only enhancement of the antibacterial activity but also improvement of the killing rate. The addition of even a small amount of α-mangostin was enough to improve the killing rate and destroy the bacterial cells. Moreover, *S. mutans* was completely killed by all mats at 180 and 240 min due to the

Table III. Kinetics Models of *In Vitro* Release Profile of Mucoadhesive Nanofiber Mats Containing Different Amounts of α-Mangostin

Nanofiber mats (% *w/w* α-mangostin)	R^2 of kinetic models		
	Zero order	First order	Higuchi
1	0.8437	0.9697	0.9808
3	0.8375	0.9739	0.9879
5	0.8812	0.9797	0.9863

Table IV. Antibacterial Susceptibility Test Results of the Mucoadhesive Nanofiber Mats Containing Different Amounts of α-Mangostin Against *S. mutans* and *S. sanguinis*

Nanofiber mats	MIC (mg/ml)		MBC (mg/ml)	
(% *w/w* α-mangostin)	*S. mutans*	*S. sanguinis*	*S. mutans*	*S. sanguinis*
0	3	2	4	3
1	2	2	3	3
3	1	1	2	2
5	0.5	0.5	1	1

longer contact between the mats and the bacterial cells. In addition, the killing rate depended on the strain of organism. The time-kill plot for *S. sanguinis* is shown in Fig. 5b. *S. sanguinis* was easier to kill and destroyed more quickly than *S. mutans*; the cells were completely killed within 120 min. These results were in agreement with a previous study that reported that these bacteria are easier to kill than oral bacteria (41). Rapid killing was observed when the cells were treated with 1, 3, or 5% α-mangostin-loaded mats at 30 and 60 min. This result confirmed that α-mangostin loading had the advantage of improving the bacterial killing rate.

Cytotoxicity Test

The cytotoxicity of α-mangostin and α-mangostin-loaded nanofiber mats was investigated in HaCaT cells and HGFs. HaCaT cells are an immortal human keratinocyte cell line that is utilized for its capacity to differentiate and proliferate *in vitro* (42). HGFs are isolated from human gingiva, so they are in close proximity to restorative dental materials in the oral cavity. The half-maximal inhibitory concentration (IC_{50}) values of α-mangostin relative to HaCaT cells and HGFs were determined, as displayed in the IC_{50} curves in Fig. 6a. The curves indicated concentration-dependent cytotoxicity following incubation for 24 h. The IC_{50} values of α-mangostin were 0.27 and 0.14 μg/ml for HaCaT cells and HGFs, respectively. These concentrations represented the concentration of α-mangostin that would be toxic to 50% of cells. HGFs were affected by a lower IC_{50} than HaCaT cells were due to the sensitivity of primary cells. The IC_{50} values for both cell types were lower than the concentration of loaded α-mangostin (26, 72, and 127 μg/ml in 4 mg/ml 1, 3, and 5% α-mangostin-loaded mats, respectively). These three concentrations may be toxic to both cell types within 24 h. Thus, the mats should be used in the oral cavity for <24 h. Given the release of α-mangostin from the mats and the results of the time-kill assay, the cytotoxicity of the mats was evaluated for 240 min.

An acute cytotoxicity test was conducted by incubation of the cells with nanofiber mats for 15, 30, 60, 120, or 240 min. The concentration of all mats was fixed at the effective bactericidal concentration (4 mg/ml). The percentage of cell viability was evaluated as presented in Fig. 6b and c. For the HaCaT cells (Fig. 6b), there was no significant decrease in cell viability when the cells were incubated with any mat type for 15, 30, 60, 120, or 240 min compared with the viability of the control. In contrast, cytotoxicity was observed when the HGFs were incubated for 120 or 240 min compared with the viability of the control ($p<0.05$) (Fig. 6c). However, no significant difference in HGF viability was observed between all mats and the control at 15, 30, or 60 min. These results indicated that the cytotoxicity of the nanofiber mats was dependent on the survival of the HGFs. The HaCaT cells and HGFs had been alive for 240 or 60 min when the cells were cultured with each mat type. Thus, the mats were safely used in the oral cavity for at least 60 min. The long-term cytotoxicity was evaluated after the cells were treated with the mats for 60 min. The cells were rinsed, the medium was replaced with SFM, and the cells were reincubated for 24, 48, or 72 h. The percentage of cell viability is displayed in Fig. 6d and e. The viability of the HaCaT cells and HGFs was not significantly different from that of the control at 24, 48, and 72 h of incubation with any type of nanofiber mat, indicating that the mats would be less cytotoxic at 72 h after using the mats for 60 min in the oral cavity.

In Vivo Test

The cytotoxicity of the α-mangostin-loaded nanofiber mats in cell culture revealed that the mats were safe for use in the oral cavity for 60 min and, after use, for 72 h. Thus, the mats should be adhered to the buccal mucosa and then removed within 60 min. Over 60 min during the time-kill assay, bacterial counts were reduced by the blank and the 1, 3, and

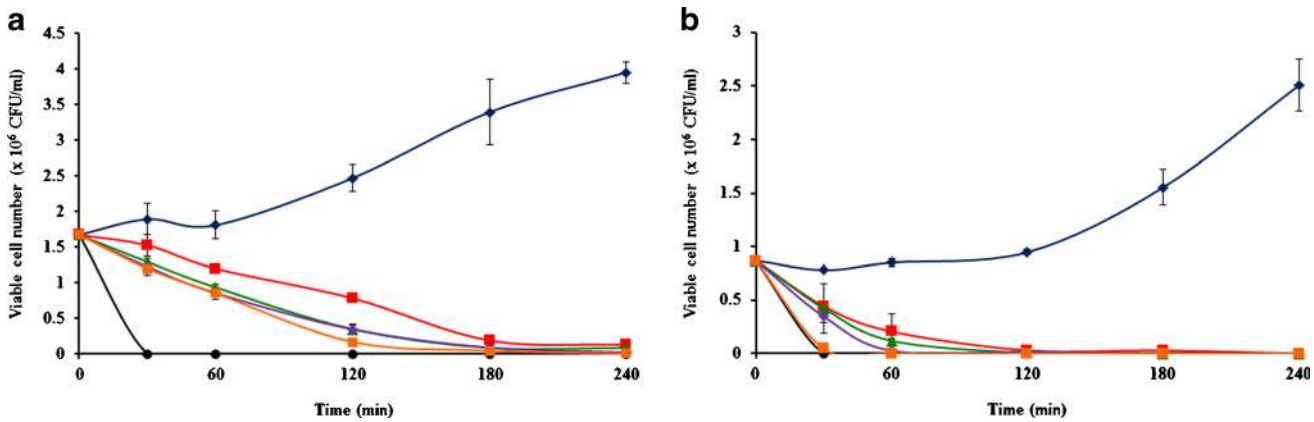

Fig. 5. Time kill plots of **a** *S. mutans* and **b** *S. sanguinis vs.* the treatment time for *blue diamond* negative control, *black circle* positive control and the 4 mg of mucoadhesive nanofiber mats containing α-mangostin: *red square* 0, *green triangle* 1, *violet diamond* 3, and *orange square* 5% *w/w* to polymer

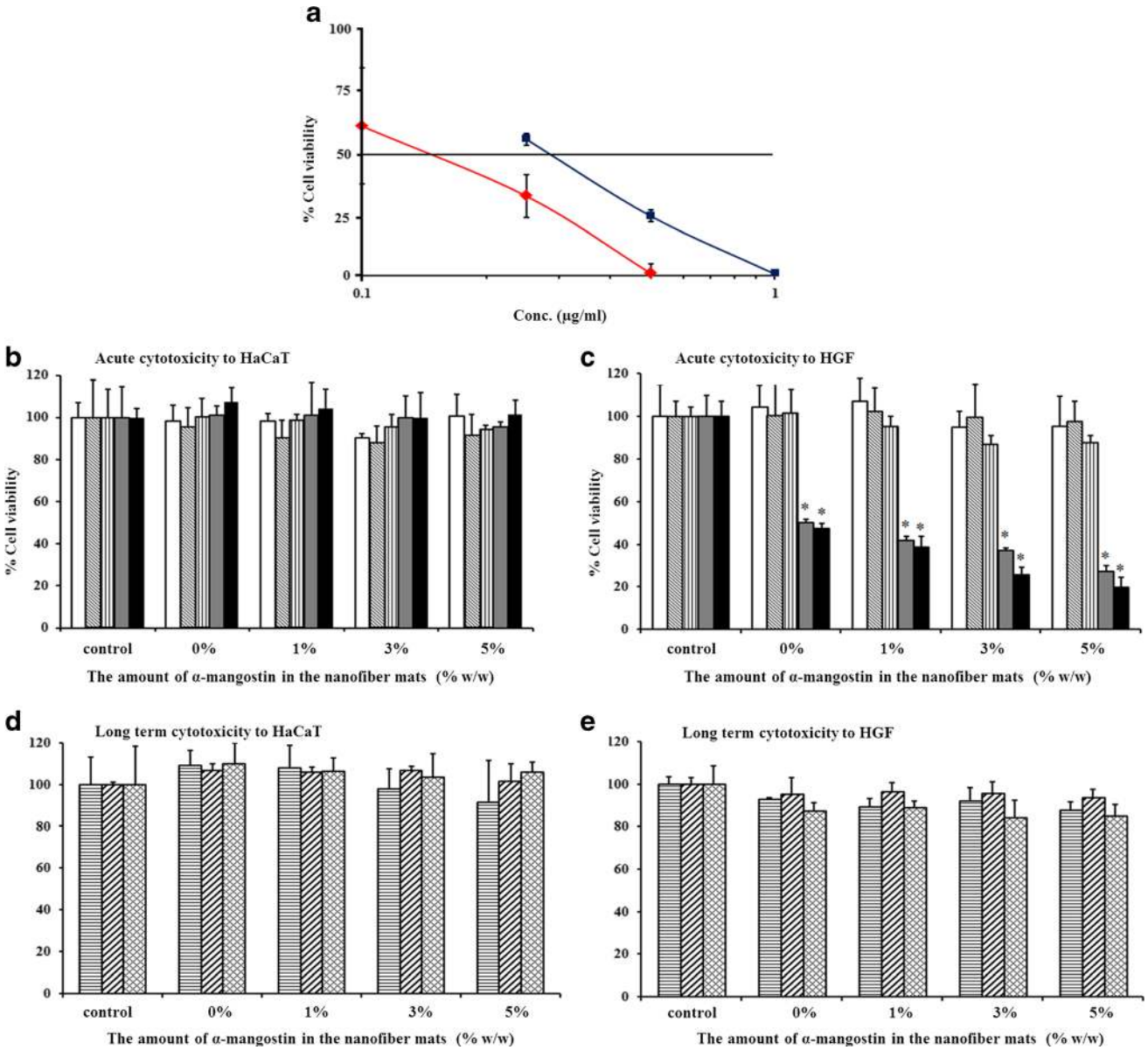

Fig. 6. **a** The percentage of cell viability among ■ HaCaT cells and ♦ HGFs in the presence of α-mangostin at 0–1 μg/ml for 24 h and the percentage of cell viability among HaCaT cells and HGFs following (**b** and **c**) acute or (**d** and **e**) long-term exposure to the mucoadhesive nanofiber mats containing different amounts of α-mangostin, serving as an indicator of cytotoxicity: incubation for □ 15, ▧ 30, ▥ 60, ▩ 120, ■ 240 min, ▤ 24, ▨ 48, and ▩ 72 h. *$p<0.05$

5% α-mangostin-loaded nanofiber mats. The α-mangostin-loaded nanofiber mats significantly decreased the number of *S. mutans* compared with the blank mats. However, there was no significant difference between the amounts of α-mangostin in the mats in terms of the bacterial activity at this time point. The addition of even a small amount of α-mangostin was enough to decrease the bacterial cell number, so the 1% α-mangostin-loaded nanofiber mats were chosen as the optimal formula to study *in vivo*. The six healthy human volunteers (three male and three female with an average age of 24.8± 4 years) were administered a 1% α-mangostin-loaded nanofiber mat for adhesion to the buccal mucosa, and the period of adhesion recorded was 5.16±1.02 min. A mat adhered to the mucosa via the mechanism described above. After that, the α-mangostin was released from the mats and then interacted with bacterial cells. Figure 7 shows the reduction in bacteria at the various time points, indicating that the mats had antibacterial activity not only *in vitro* but also *in vivo*. When a mat adhered to the buccal mucosa for 5 min and then detached, the antibacterial activity had been occurring for 60 min. The number of viable bacterial cells was significantly decreased at all sampling times compared with the number before using the mat. A 70% reduction in *Streptococcus* spp. and *Lactobacillus* spp. from baseline occurred after using the mat for 60 min. Bitterness was not observed, and smoothness was maintained during the test. These results indicated that this mat provided mucoadhesive properties, antibacterial activity in the oral cavity, and a good taste and a good mouth feel. The cytotoxicity of

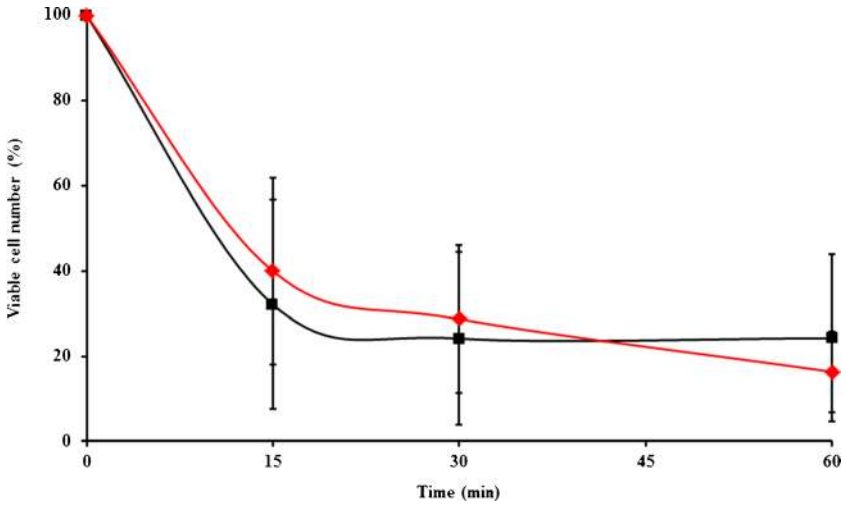

Fig. 7. The reduction of bacterial cells at various time points in the oral cavity when using 1% w/w α-mangostin-loaded nanofiber mats: *square Streptococcus* spp. and *diamond Lactobacillus* spp.

the α-mangostin-loaded nanofiber mats in cell culture revealed that the mats were safe for use in the oral cavity for 60 min and, after use, for 72 h. Thus, the mats should be adhered to the buccal mucosa and then removed within 60 min. Over 60 min during the time-kill assay, bacterial counts were reduced by the blank and the 1, 3, and 5% α-mangostin-loaded nanofiber mats. The α-mangostin-loaded nanofiber mats significantly decreased the number of *S. mutans* compared with the blank mats. However, there was no significant difference between the amounts of α-mangostin in the mats in terms of the bacterial activity at this time point. The addition of even a small amount of α-mangostin was enough to decrease the bacterial cell number, so the 1% α-mangostin-loaded nanofiber mats were chosen as the optimal formula to study *in vivo*. The six healthy human volunteers (three male and three female with an average age of 24.8± 4 years) were administered a 1% α-mangostin-loaded nanofiber mat for adhesion to the buccal mucosa, and the period of adhesion recorded was 5.16±1.02 min. A mat adhered to the mucosa via the mechanism described above. After that, the α-mangostin was released from the mats and then interacted with bacterial cells. Figure 7 shows the reduction in bacteria at the various time points, indicating that the mats had antibacterial activity not only *in vitro* but also *in vivo*. When a mat adhered to the buccal mucosa for 5 min and then detached, the antibacterial activity had been occurring for 60 min. The number of viable bacterial cells was significantly decreased at all sampling times compared with the number before using the mat. A 70% reduction in *Streptococcus* spp. and *Lactobacillus* spp. from baseline occurred after using the mat for 60 min. Bitterness was not observed, and smoothness was maintained during the test. These results indicated that this mat provided mucoadhesive properties, antibacterial activity in the oral cavity, and a good taste and a good mouth feel.

Stability Studies

The remaining α-mangostin content in the nanofiber mats was determined after maintenance under long-term conditions (25±2°C and 60±5% RH) or accelerated conditions (40±2°C and 75±5% RH) for 6 months. The α-mangostin content, reflected by the loading efficacy and capacity, is shown in Table V. There was no significant difference in loading efficacy or capacity between the time points or conditions of storage. However, a large standard deviation in the loading efficacy at 3 and 6 months of storage was observed, without a significant difference in loading efficacy between these time points, indicating variation in α-mangostin content after storage that was possibly caused by the temperature and humidity of the storage conditions. From the results, it can be assumed that the nanofiber mats were stable for at least 6 months.

CONCLUSION

α-Mangostin was successfully incorporated into the synthesized CS-SH/PVA nanofiber mats via the electrospinning process. The fiber mats provided suitable properties, i.e., in terms of diameter, tensile strength, swelling, mucoadhesion, and stability.

Table V. The Loading Efficacy and Capacity (%) of α-Mangostin in the 1% α-Mangostin Loaded Nanofiber Mats After Keeping Under Long-Term Condition Comparing with Accelerated Condition for 6 months

	Loading efficacy (%)		Loading capacity (%)	
Stored for (month)	Long term	Accelerated	Long term	Accelerated
1	68.84±0.53	69.60±0.53	0.682±0.054	0.689±0.005
3	70.48±6.08	71.19±7.32	0.698±0.060	0.704±0.072
6	69.25±8.28	71.66±0.48	0.686±0.082	0.710±0.005

These mats were non-toxic, with a good mouth feel, in the oral cavity and rapidly adhered to the buccal, after which the α-mangostin was released to destroy oral bacteria, reducing their number. Therefore, these nanomaterials may be promising candidates for the maintenance of oral hygiene and reduction of the bacterial growth that can develop from dental caries.

ACKNOWLEDGMENTS

The authors wish to thank the Commission of Higher Education (Thailand), the Thailand Research Funds through the Royal Golden Jubilee PhD Program (Grant No. PHD/0001/2553) and the Silpakorn University Research and Development Institute for financial support, Associate Professor Suchada Chutimaworapan for her support, and Ms Kusuma Jamdee and Ms Niratcha Chaisomboon for technical guidance.

REFERENCES

1. Wang W, Tao R, Tong Z, Ding Y, Kuang R, Zhai S, *et al*. Effect of a novel antimicrobial peptide chrysophsin-1 on oral pathogens and *Streptococcus mutans* biofilms. Peptides. 2012;33:212–9.
2. Loesche WJ. Role of *Streptococcus mutans* in human dental decay. Microbiol Rev. 1986;50:353–80.
3. Quivey RG, Kuhnert WL, Hahn K. Genetics of acid adaptation in oral *streptococci*. Crit Rev Oral Biol Med. 2001;12:301–14.
4. Kim JE, Kim HE, Hwang JK, Lee HJ, Kwon HK, Kim BI. Antibacterial characteristics of *Curcuma xanthorrhiza* extract on *Streptococcus mutans* biofilm. J Microbiol. 2008;46(2):228–32.
5. Keohane J, Ryan K, Shanahan R. *Lactobacillus* in gastrointestinal tract. In: Ljungh A, Wadstrom T, editors. *Lactobacillus* molecular biology: from genomics to probiotics. Norfolk: Caister Academic Press; 2009. p. 169–82.
6. American Academy of Pediatric Dentistry, Pediatric dentistry, Reference manual 2009–2010;31(6):10.
7. Ashkenazi M, Bidoosi M, Levin L. Factors associated with reduced compliance of children to dental preventive measures. Odontology. 2012;100:241–8.
8. Sakagami Y, Iinuma M, Piyasena KGNP, Dharmaratne HRW. Antibacterial activity of α-mangostin against vancomycin resistant *Enterococci* (VRE) and synergism with antibiotics. Phytomedicine. 2005;12:203–8.
9. Chomnawang MT, Surassmo S, Wongsariya K, Bunyapraphatsara N. Antibacterial activity of Thai medicinal plants against methicillin-resistant *Staphylococcus aureus*. Fitoterapia. 2009;80:102–4.
10. Sudhakar Y, Kuotsu K, Bandyopadhyay AK. Buccal bioadhesive drug delivery—a promising option for orally less efficient drugs. J Control Release. 2006;114:15–40.
11. Langoth N, Kahlbacher H, Schöffmann G, Schmerold I, Schuh M, Franz S, *et al*. Thiolated chitosans: design and in-vivo evaluation of a mucoadhesive buccal peptide drug delivery system. Pharm Res. 2006;23(3):573–9.
12. Bernkop-Schnürch A, Hornof M, Guggi D. Thiolated chitosans. Eur J Pharm Biopharm. 2004;57:9–17.
13. Langoth N, Kalbe J, Bernkop-Schnürch A. Development of buccal drug delivery systems based on a thiolated polymer. Int J Pharm. 2003;252:141–8.
14. Marschütz MK, Bernkop-Schnürch A. Thiolated polymers: self-crosslinking properties of thiolated 450 kDa poly(acrylic acid) and their influence on mucoadhesion. Eur J Pharm Sci. 2002;15:387–94.
15. Samprasit W, Kaomongkolgit R, Sukma M, Rojanarata T, Ngawhirunpat T, Opanasopit P. Mucoadhesive electrospun chitosan-based nanofiber mats for dental caries prevention. Carbohydr Polym. 2015;117:933–40.
16. Morales JO, McConville JT. Manufacture and characterization of mucoadhesive buccal films. Eur J Pharm Biopharm. 2011;77:187–99.
17. Huang ZM, Zhang YZ, Kotaki M, Ramakrishna S. A review on polymer nanofibers by electrospinning and their applications in nanocomposites. Compos Sci Technol. 2003;63:2223–53.
18. Kaomongkolgit R, Jamdee K, Chaisomboon N. Antifungal activity of alpha-mangostin against *Candida albicans*. J Oral Sci. 2009;51(3):401–6.
19. Schmitz T, Grabovac V, Palmberger TF, Hoffer MH, Bernkop-Schnürch A. Synthesis and characterization of a chitosan-*N*-acetyl cysteine conjugate. Int J Pharm. 2008;347:79–85.
20. Thirawong N, Nunthanid J, Puttipipatkhachorn S, Sriamornsak P. Mucoadhesive properties of various pectins on gastrointestinal mucosa: an in-vitro evaluation using texture analyzer. Eur J Pharm Biopharm. 2007;67:132–40.
21. Pothitirat W, Chomnawang MT, Supabphol R, Gritsanapan W. Comparison of bioactive compounds content, free radical scavenging and anti-acne inducing bacteria activities of extracts from the mangosteen fruit rind at two stages of maturity. Fitoterapia. 2009;80:442–7.
22. Hadjiioannou T, Christian G, Koupparis M, Macheras P. Quantitative calculations in pharmaceutical practice and research. New York: VCH Publishers Inc; 1993.
23. Bourne D. Pharmacokinetics. In: Banker G, Rhodes C, editors. Modern pharmaceutics. New York: Marcel Dekker Inc.; 2002. p. 67–92.
24. Higuchi T. Mechanism of sustained-action medication. Theoretical analysis of rate of release of solid drugs dispersed in solid matrices. J Pharm Sci. 1963;52:1145–9.
25. Jorgensen JH, Turnidge JD. Antibacterial susceptibility tests: dilution and disk diffusion methods. In: Murray PR, Baron EJ, Jorgensen JH, Landry ML, Pfaller MA, editors. Manual of clinical microbiology. Washington DC: American Society for Microbiology; 2007. p. 1152–72.
26. Hindler JA. Special antimicrobial susceptibility test. In: Mahon CR, Manuselis G, editors. Textbook of the diagnostic microbiology. Philadelphia: WB Saunders; 2000. p. 97–104.
27. Sreenivas SA, Pai KV. Thiolated chitosans: novel polymers for mucoadhesive drug delivery—a review. Trop J Pharm Res. 2008;7(3):1077–88.
28. Thompson CJ, Chase GG, Yarin AL, Reneker DH. Effects of parameters on nanofiber diameter determined from electrospinning model. Polymer. 2007;48:6913–22.
29. Bhardwaj N, Kundu SC. Electrospinning: a fascinating fiber fabrication technique. Biotechnol Adv. 2010;28:325–47.
30. Zong X, Kim K, Fang D, Ran S, Hsiao BS, Chu B. Structure and process relationship of electrospun bioabsorbable nanofiber membranes. Polymer. 2002;43:4403–12.
31. Smart JD. The basics and underlying mechanisms of mucoadhesion. Adv Drug Deliv Rev. 2005;57:1556–68.
32. Salamat-Miller N, Chittchang M, Johnston TP. The use of mucoadhesive polymers in buccal drug delivery. Adv Drug Deliv Rev. 2005;57:1666–91.
33. Aisha AFA, Ismail Z, Abu-Salah KM, Majid AMSA. Solid dispersions of α-mangostin improve its aqueous solubility through self-assembly of nanomicelles. J Pharm Sci. 2012;101:815–25.
34. Sill TJ, Recum HA. Electrospinning: applications in drug delivery and tissue engineering. Biomaterials. 2008;29:1989–2006.
35. Nagy ZK, Nyúl K, Wagner I, Molnár K, Marosi G. Electrospun water soluble polymer mat for ultrafast release of Donepezil HCl. Express Polym Lett. 2010;4(12):763–72.
36. Tong Z, Zhou L, Li J, Jiang W, Ma L, Ni L. In-vitro evaluation of the antibacterial activities of MTAD in combination with Nisin against *Enterococcus faecalis*. J Endod. 2011;37:1116–20.
37. Koh JJ, Qiu S, Zou H, Lakshminarayanan R, Li J, Zhou X, *et al*. Rapid bactericidal action of alpha-mangostin against MRSA as an outcome of membrane targeting. Biochim Biophys Acta. 2013;1828:834–44.
38. El-Sharif AA, Hussain MHM. Chitosan–EDTA new combination is a promising candidate for treatment of bacterial and fungal infections. Curr Microbiol. 2011;62:739–45.

39. Banin E, Brady KM, Greenberg EP. Chelator-induced dispersal and killing of *Pseudomonas aeruginosa* cells in a biofilm. Appl Environ Microbiol. 2006;72(3):2064–9.
40. Eckert R, Qi F, Yarbrough DK, He J, Anderson MH, Shi W. Adding selectivity to antimicrobial peptides: rational design of a multidomain peptide against *Pseudomonas* spp. Antimicrob Agents Chemother. 2006;50:1480–8.
41. Li F, Weir MD, Fouad AF, Xu HHK. Time-kill behaviour against eight bacterial species and cytotoxicity of antibacterial monomers. J Dent. 2013;41:881–91.
42. Schürer N, Köhne A, Schliep V, Barlag K, Goerz G. Lipid composition and synthesis of HaCaT cells, an immortalized human keratinocyte line, in comparison with normal human adult keratinocytes. Exp Dermatol. 1993;2(4):179–85.